

Octadecyl and sulfonyl modification of diatomite synergistically improved the immobilization efficiency of lipase and its application in the synthesis of pine sterol esters

Yifei Zhang¹, Wei Zhang¹, Guangzheng Ma¹, Binbin Nian¹, and Yi Hu¹

¹Nanjing Tech University

November 9, 2023

Abstract

Phytosterols usually have to be esterified to various phytosterol esters to avoid their disadvantages of unsatisfactory solubility and low bioavailability. The enzymatic synthesis of phytosterol esters in solvent-free system has advantages in terms of environmental friendliness, sustainability, and selectivity. However, the limitation of the low stability and recyclability of the lipase in the solvent-free system, which often requires a relatively high temperature to induce the viscosity, also increased the industrial production cost. In this context, a low-cost material, namely diatomite, was employed as the support in the immobilization of *Candida rugosa* lipase (CRL) due to its multiple modification sites. The Fe₃O₄ was also then introduced to this system for quick and simple separation via the magnetic field. Moreover, to further enhance the immobilization efficiency of diatomite, a modification strategy which involved the octadecyl and sulfonyl group for regulating the hydrophobicity and interaction between the support and lipase was successfully developed. The optimization of the ratio of the modifiers suggested that the -SO₃H/C₁₈ (1:1.5) performed best with an enzyme loading and enzyme activity of 84.8 mg·g⁻¹ and 54 U·g⁻¹, respectively. Compared with free CRL, the thermal and storage stability of CRL@OSMD was significantly improved, which lays the foundation for the catalytic synthesis of phytosterol esters in solvent-free systems. Fortunately, a yield of 95.0% was achieved after optimizing the reaction conditions, and a yield of 70.0% can still be maintained after 6 cycles.

Octadecyl and sulfonyl modification of diatomite synergistically improved the immobilization efficiency of lipase and its application in the synthesis of pine sterol esters

Yifei Zhang, Wei Zhang, Guangzheng Ma, Binbin Nian* and Yi Hu*

(State Key Laboratory of Materials-Oriented Chemical Engineering, School of Pharmaceutical Sciences, Nanjing Tech University, Nanjing, China)

Abstract

Phytosterols usually have to be esterified to various phytosterol esters to avoid their disadvantages of unsatisfactory solubility and low bioavailability. The enzymatic synthesis of phytosterol esters in solvent-free system has advantages in terms of environmental friendliness, sustainability, and selectivity. However, the limitation of the low stability and recyclability of the lipase in the solvent-free system, which often requires a relatively high temperature to induce the viscosity, also increased the industrial production cost. In this context, a low-cost material, namely diatomite, was employed as the support in the immobilization of *Candida rugosa* lipase (CRL) due to its multiple modification sites. The Fe₃O₄ was also then introduced to this system for quick and simple separation via the magnetic field. Moreover, to further enhance the immobilization efficiency of diatomite, a modification strategy which involved the octadecyl and sulfonyl group for regulating the hydrophobicity and interaction between the support and lipase was successfully developed. The optimization of the ratio of the modifiers suggested that the -SO₃H/C₁₈ (1:1.5) performed best with an

enzyme loading and enzyme activity of $84.8 \text{ mg}\cdot\text{g}^{-1}$ and $54 \text{ U}\cdot\text{g}^{-1}$, respectively. Compared with free CRL, the thermal and storage stability of CRL@OSMD was significantly improved, which lays the foundation for the catalytic synthesis of phytosterol esters in solvent-free systems. Fortunately, a yield of 95.0% was achieved after optimizing the reaction conditions, and a yield of 70.0% can still be maintained after 6 cycles.

Keywords: *Candida rugosa* lipase, diatomite, octadecyl and sulfonyl modification, immobilization, phytosterol esters

Graphical abstract

Introduction

Sterols are lipids that play a crucial role in all multicellular eukaryotes. The distribution and synthesis of sterols varies among the eukaryotic community, with animals primarily producing cholesterol (C_{27}), whereas fungi and plants synthesis sterols with 28 to 29 carbon atoms (C_{28} and C_{29}), known as ergosterols and phytosterols[1, 2]. These differences reflect the complex evolutionary history of sterol synthesis[3]. Phytosterols, which include phytostanols and sterols, are similar in structure and biological function to cholesterol[4, 5]. They are primarily found in vegetable oils, nuts, fruits, grains, and other plant products[6]. Phytosterols have been recognized for their various pharmacological properties, including the potential to lower total and low-density lipoprotein (LDL) cholesterol levels, thereby reducing the risk of cardiovascular disease[7-9]. Other health-promoting effects of phytosterols include anti-obesity[10], anti-diabetic[9], anti-microbial[11], anti-inflammatory[12], and immunomodulatory effects[13]. Additionally, it has been strongly suggested that phytosterols possess anti-cancer properties, as phytosterol-rich diets may reduce the risk of cancer by 20%[14, 15]. However, the high melting point and low solubility in both water and oils have greatly limited their further application in food, medicine, and other fields. To overcome this problem, phytosterol esters are considered suitable alternatives because they maintain all the excellent properties of original phytosterol[16, 17].

The chemical synthesis of phytosterol esters is industrially feasible, but the high energy consumption, low selectivity of the reaction, and the unavoidable by-products of dehydrated sterols limit its further applications[18]. Enzymatic catalysis which is performed under mild operating conditions, has high selectivity and fewer by-products and is therefore attractive in this field[19]. In recent years, several lipases, including Novozym[®] 435[20], *Candida rugosa* lipase[21], and others, have demonstrated their ability in the synthesis of phytosterol esters. However, these reactions usually were performed in organic solvents, which limited the space-time yield and were harmful to the enzymes. To overcome the damage of organic solvent, some environmentally friendly mediums, such as ionic liquids[22], and supercritical carbon dioxide[23] were applied in biocatalysis. In this work, the esterification process is performed in a solvent-free system. However, we just found that the solvent-free system's high viscosity limited the substrates' mass-transfer effect, which made the reaction time extremely long. It indicated that the reaction can only be performed at a relatively higher temperature (50), which may not be beneficial to the lipase.

In response to this challenge, the immobilization of enzymes that aimed to improve stability and recyclability has attracted more and more interest, and various immobilization methods and supports with low cost, large specific surface area, and low diffusion limits of substrates, have been developed in past decades. For instance, diatomite, which is mainly composed of silicon dioxide (SiO_2), was widely used in the immobilization of various enzymes due to its low cost, porous structure, low density, and chemical inertness. Chen et al.[24] suggested that the half-lives of diatomite immobilized of D-allulose 3-epimerase can be improved to 109 and 124 times than that of free enzyme at 55 and 60, respectively. Polyaniline-coated magnetic diatomite can efficiently immobilize invertase, β -galactosidase, and trypsin[25]; *Candida* sp. 99-125 immobilized on diatomite can be used to produce biodiesel efficiently[26]; *Burkholderial* lipase immobilized on diatomite can be applied to a fixed-bed bioreactor and continuous biodiesel conversion[27]. However, single immobilization support does not meet the needs of all enzymes, therefore, for the immobilization of different enzymes, different modifiers need to be designed to confer a more suitable microenvironment to the support as well as the strength of interaction with the enzyme, e.g., basso's study indicated that the octadecyl functional group can

change the hydrophobic microenvironment of lipase, which can have a significant effect on the enzyme activity[28], and Singh modified the surface of silica nanoparticles with carboxylic acids with different numbers of alkyl chains, and found that silica-immobilized lipase modified by stearic acid with more hydrophobicity has a higher activity[29]. Moreover, the production of water during the esterification reactions will drive the reaction toward hydrolysis and lead to enzyme inactivation via promoting the aggregation of enzymes[30, 31]. Additionally, it will also accelerate the leakage of lipase from the support during reutilization.

Therefore, to develop a low-cost, sustainable, and high-efficiency enzymatic synthesis strategy for phytosterol esters, the solvent-free system was applied in the present study. To overcome the challenge of the low stability of lipase, a cheap inorganic porous material, namely diatomite was applied as a support for the immobilization of *Candida rugosa* lipase (CRL). To further enhance its efficiency, the magnetic nano-Fe₃O₄ was first attached to the surface of diatomite via a co-precipitation method. Moreover, the octadecyl and sulfonyl groups were applied as modifiers of the diatomite for regulating its hydrophobicity, flexibility, and interaction and thus improve the efficiency of diatomite. Additionally, the immobilized enzyme prepared by this method was used in the enzymatic synthesis of phytosterol esters to test its stability and recyclability. This study is anticipated to provide a green and efficient innovative method for the enzymatic synthesis of phytosterol esters.

2. Materials and Methods

2.1. Materials

Pine sterol (91.0% β -sitosterol, 7.0% campesterol, 0.5% stigmasterol, 0.3% brassicasterol, and 1.2% others) was kindly donated from Jiangsu Conat Biological Products Co., Ltd (Jiangsu, China); diatomite (200 mesh) was purchased from Aladdin (Shanghai, China); FeCl₃·6H₂O, FeCl₂·4H₂O, 3-mercaptopropyltriethoxysilane (97%), n-octadecyltriethoxysilane (85%), Oleic acid (99.0%) were purchased from Sarn Chemical Technology Co., Ltd (Shanghai, China). *Candida rugosa* lipase (type VII) was purchased from Sigma-Aldrich (St. Louis, MO, USA).

2.2 Preparation and modification of magnetic diatomite

4.1 g of FeCl₃·6H₂O and 2.6 g of FeCl₂·4H₂O were dissolved in a quantity of deionized water and mixed ultrasonically. After sufficient shaking, 6.0 g of diatomaceous earth was added and stirred at 80 °C for 30 min using nitrogen protection. Add ammonia, adjust pH to 10, and continue mixing for 1 h. Cooling slowly to room temperature and crystallize for 2 h. The precipitate obtained after magnetic field separation was sequentially washed with deionized water and ethanol. After drying, magnetic diatomite (MD) was obtained.

1.0 g of MD was added to 50.0 mL of toluene, sonicated, and mixed for 0.5 h. After that, 0.8-2.4 g of 3-mercaptopropyltriethoxysilane and 1.4-4.2 g of n-octadecyltriethoxysilane were added. Using nitrogen protection, the reaction was heated to reflux for 12 hours. Then, the diatomite was separated by a magnetic field, washed several times with ethanol, and the product was dried under vacuum at 45°C to obtain octadecyl and thiol co-bonded magnetic diatomite. The obtained octadecyl and thiol co-bonded magnetic diatomite was added to a certain concentration of H₂O₂ and stirred at 40°C for 24 h and then washed with water to remove the excess H₂O₂. After drying under vacuum at 60°C, octadecyl and sulfonyl co-bonded magnetic diatomite (OSMD) was obtained.

2.3 Immobilization of *Candida rugosa* lipase

The aqueous lipase solution was centrifuged at 4025 xg for 10 min at 4°C to remove the insoluble material to obtain a homogeneous semi-purified lipase. The resulting supernatant was separated and used for subsequent experiments.

As different supports have their suitable immobilization conditions, it is reasonable to compare the immobilization effect of the supports on this basis. 0.1 g of modified magnetic diatomite was added to 5 mL of semi-purified CRL with different concentrations and different pH values (6.0-8.0) and then stirred at 25-40°C for 4-12 h. After filtration under reduced pressure, washing, and freeze drying, the immobilized enzyme pro-

duct was obtained. Enzyme loading and immobilization efficiency are important parameters that define the immobilization process. Enzyme loading is an important parameter to examine the loading capacity of the support, and immobilization efficiency (immobilization yield) is usually employed to define the percentage of the enzyme that is immobilized on or in the support.

The BCA method was used to detect the protein content in the supernatant. All the measurements were done in triplicate and the error was less than 5% in each case, and the following formula was used to calculate CRL loading and immobilization efficiency.

$$\text{CRL loading} \left(\frac{\text{mg}}{\text{g}} \right) = \frac{C_i \times M_i - C_f \times V_f}{M_f} \# (1)$$

$$\text{Immobilization efficiency} (\%) = \frac{C_i \times M_i - C_f \times V_f}{C_i \times M_i} \times 100 \# (2)$$

where C_i (mg/g) is the initial protein concentration in CRL before immobilization, C_f (mg/mL) is the final protein concentration in supernatant and washing solution after immobilization, M_i (mg) is the mass of CRL added to the buffer solution, V_f (mL) is the total volume of the supernatant and washing liquid, and M_f (g) is the mass of the support.

2.4 Enzyme activity assay

The expressed activity gives the enzyme activity expressed by the immobilized enzyme itself and the specific activity shows the effect of the immobilization process on the enzyme activity, these two parameters together with the enzyme loading and the immobilization efficiency form the parameters required to define the immobilization process[32].

The p-nitrophenyl palmitate (p-NPP) assay has been widely used to analyze lipase activity[33, 34]. One unit (1 U) is defined as the amount of enzyme required to catalyze the hydrolysis of p-nitrophenyl palmitate to produce 1 μmol of p-nitrophenol per minute at 40°C and pH 7.0. All the measurements were done in triplicate and the error was less than 5% in each case.

The activity of CRL (immobilized CRL) and activity recovery were calculated by the following equation:

$$\text{Expressed activity} (Ug^{-1}) = \frac{A \times 10^6 \times V_t}{\varepsilon \times t \times m_1} \# (3)$$

$$\text{Specific activity} (Ug^{-1}) = \frac{A \times 10^6 \times V_t}{\varepsilon \times t \times m_2} \# (4)$$

$$\text{Activity recovery} (\%) = \frac{SA_1}{SA_0} \times 100 \# (5)$$

Where A is the absorbance of the samples, V_t (L) is the volume of the solution, ε ($\text{L} \cdot \text{mol}^{-1} \cdot \text{cm}^{-1}$) is the molar extinction coefficient of p-nitrophenol, t (min) is the reaction time, m_1 (g) is the mass of immobilized CRL and m_2 (g) is the protein mass of immobilized CRL, SA_1 ($\text{U} \cdot \text{g}^{-1}$) is the specific activity of immobilization CRL, SA_0 ($\text{U} \cdot \text{g}^{-1}$) is the specific activity of free CRL.

The following formula was used to calculate relative activity and residual activity.

$$\text{Relative activity} (\%) = \frac{A_t}{A_{\max}} \times 100 \# (6)$$

$$\text{Residual activity} (\%) = \frac{A_t}{A_i} \times 100 \# (7)$$

Where A_t is the absorbance of the samples, A_{\max} is the maximum absorbance, and A_i is the initial absorbance value of the samples.

2.5 Characterizations

Scanning electron microscopy (SEM) was performed on a Hitachi FE-SEM SU8200 instrument (Japan). Thermogravimetric analysis (TGA) was performed on a TGA 550 instrument (TA Instruments, USA) at 20-800°C under N₂ atmosphere using a heating rate of 20°C/min. The FTIR spectra of the MD and OSMD samples were measured using Nicolet iS50 FT-IR (Thermo Scientific, USA). Spectra were taken from 4000 to 400 cm⁻¹ and the resolution of the wavenumber was 2 cm⁻¹. XPS of raw diatomite and OSMD was carried out by ESCALAB250Xi (Thermo Scientific, USA). The magnetization of the immobilized enzyme was carried out by Lake Shore VSM 7307 (Lake Shore, USA). N₂ adsorption and desorption study was performed on the ASAP 2020Plus HD88 (Micromeritics, USA). Water contact angle measurement of the samples was measured with a KRUSS drop shape analyzer DSA 100 instrument at 25degC for the support and the injecting syringe as well.

2.6 Optimization of conditions for the synthesis of pine sterol oleate

Using the immobilized CRL as a catalyst, the process conditions such as the amount of catalyst, the molar ratio of the substrate between pine sterol and oleic acid, reaction time, and reaction temperature were optimized for the synthesis of pine sterol oleate by direct esterification of pine sterol with oleic acid. In a 15 mL reaction tube on an automatic temperature-controlled magnetic stirrer, 1.0 mmol of pine sterol, and 4.0-8.0 mmol of oleic acid were added as substrate, catalyzed by the immobilized enzyme of 5.0-9.0 U*g⁻¹(relative to pine sterol mass), and the reaction temperature was 35-55degC for 12-60 h.

2.7 Gas Chromatography Analysis

The quantitative analysis of pine sterol and sterol ester was performed by gas chromatography (GC) with FID detector and dichloromethane as the solvent, using a DB-5HT (0.1 μm, 0.25×15 m) column with N₂ as the carrier gas and a flow rate of 1.5 mL/min. The inlet temperature and detector temperature were 350°C, and the initial temperature of the column temperature chamber was 180°C, ramped up to 240°C at 10°C/min. The sample volume was 1 μL and the shunt ratio was 20:1.

2.8 Substrate scope investigation

To demonstrate the substrate range of CRL@OSMD, the esterification of pine sterol with oleic, linoleic, linolenic acid, and mixed acid (oleic, linoleic, and linolenic acids in equimolar ratios) was studied under optimized reaction conditions.

2.9 Process scale-up and reusability studies

To explore the scalability of the immobilized CRL-catalyzed pine sterol ester synthesis process, the feed volume was increased up to 10 times under optimized reaction conditions. The synthesis of pine sterol esters was investigated for reusability under optimized conditions. At the end of the reaction, the immobilized enzyme was filtered, separated from the reaction system, and washed with 5 mL hexane 3 times. After drying, the resulting immobilized CRL was used directly in the next batch.

3. Results and discussion

3.1 Characterization of modified diatomite

The surface morphology and elemental analysis of OSMD and CRL were characterized by SEM (**Figure 1**). The Energy Dispersive Spectroscopy (EDS) image (**Figure S1**) showed that the OSMD surface was rich in C, S, and Fe elements, which proved the success of the surface modification. After immobilizing CRL, the proportions of S and N elements increased significantly, indicating that the support could load CRL efficiently (**Figure S2**). The OSMD still retained the original unique porous structure of diatomite after the introduction of functional groups and Fe₃O₄. Obviously, the surface of immobilized CRL showed a rough morphology, indicating that CRL was efficiently immobilized on the surface of the support.

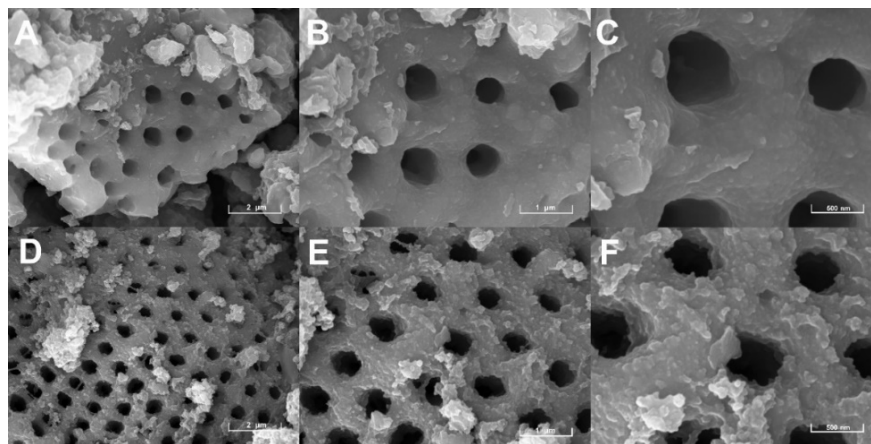


Figure 1 . SEM images of OSMD (A, B, C) and CRL@OSMD (D, E, F)

Figure 2. A shows the FTIR spectra of the original diatomite, MD, and OSMD. According to the FTIR diagram of the raw diatomite, the absorption peaks of 3622.3 cm^{-1} , 3450.0 cm^{-1} , and 1639.7 cm^{-1} are formed by the stretching vibration of $-\text{OH}$. The absorption peaks at 1025.2 and 792.4 cm^{-1} correspond to the stretching vibration of Si-O-Si ; the bending vibration of the Si-O bond forms the absorption peak at 451.2 cm^{-1} . Instead, there are some new peaks in the FTIR of modified diatomite. The absorption peaks at 2925.5 cm^{-1} , 2850.1 cm^{-1} , and 1463.1 cm^{-1} in the infrared spectrum of modified diatomite correspond to the stretching vibration and bending vibration of the C-H bond in $-\text{C}_{18}$, which is consistent with the study of Li et al[35]. The peak at around 1396.5 cm^{-1} and 1140.0 cm^{-1} is caused by the vibration of S=O in $-\text{SO}_3\text{H}$. The surface modification of the diatomite with alkyl groups can be demonstrated by the Si-C associated peaks appearing at 720.3 cm^{-1} , which is consistent with the work reported by Xu et al[36]. All the above results indicated that the diatomite was successfully modified.

The magnetization of OSMD and CRL@OSMD was measured using a Vibrating Sample Magnetometer (VSM) at room temperature (**Figure 2. B**). The remanent magnetization and coercivity of OSMD and CRL@OSMD were almost zero, indicating that the sample materials are soft magnetic materials with superparamagnetic and outstanding magnetic properties[37]. The specific saturation magnetization of OSMD and CRL@OSMD were $12.2\text{ emu}\cdot\text{g}^{-1}$ and $12.1\text{ emu}\cdot\text{g}^{-1}$, respectively. There is almost no difference between the two, which indicates that the immobilization process does not affect the magnetic properties of the support. The exceptional magnetic response helps to recover the immobilized enzyme under the application of a magnetic field, providing valuable support for the reuse of biocatalysts.

In addition, we employed the N_2 adsorption-desorption isotherms to provide evidence for the successful immobilization of CRL to the OSMD (**Figure 2. C**). As shown in **Figure 2.D**, the overall pore size of CRL@OSMD was significantly decreased compared to OSMD which may be attributed to that the CRL immobilized into the pore of OSMD and thus decreased the pore size of it. Moreover, the results showed that the Brunauer-Emmett-Teller (BET) surface area of OSMD decreased from $53.6\text{ m}^2\cdot\text{g}^{-1}$ to $27.2\text{ m}^2\cdot\text{g}^{-1}$ after the immobilization process, accompanied by a corresponding reduction in pore volume from $0.227\text{ cm}^3\cdot\text{g}^{-1}$ to $0.176\text{ cm}^3\cdot\text{g}^{-1}$ (**Table S1**). These findings indicate that a substantial portion of the enzyme occupies the diatomite channels, thereby achieving the effective immobilization of CRL on OSMD.

Figure 2 . FTIR spectrum of diatomite before and after modification (A), VSM plot (B), N_2 adsorption and desorption isotherms of OSMD and CRL@OSMD (C), BJH-plot (D)

Figure 3 compares the XPS spectra of OSMD, MD, and raw diatomite. The peaks of 100.1 eV ($\text{Si } 2\text{p}$), 259.2 eV ($\text{O } 1\text{s}$), and 150.5 eV ($\text{Si } 2\text{s}$) are formed by the diatomite, and the peak intensity is significantly weakened after modification, which corroborates the change in the surface groups of the diatomite. Relatively, the peak intensity of $\text{C } 1\text{s}$ (281.8 eV) was significantly enhanced after modification. Despite the weak intensity,

the peak at around 161.0 eV (S 2p) and 225.0 eV (S 2s) is caused by $-\text{SO}_3\text{H}$. Compared to raw diatomite, nanomagnetic Fe_3O_4 increased the peaks located at 710.5 eV and 719.9 eV[35]. **Table 1** shows that the C peak intensity of modified diatomite is significantly enhanced, and the content of C is increased from 15.8% to 66.1%. However, the intensity of the O1s peak weakened, and the O content decreased from 61.8% to 22.6%. It is proved that the coating contains a large amount of $-\text{C}_{18}$, and $-\text{SO}_3\text{H}$ successfully modified diatomite. In the high-resolution diagram of Si 2p, the electron absorption peaks at 100.4 eV and 99.8 eV correspond to the Si-O bond and Si-Si bond in diatomite[38]. Compared with unmodified diatomite and MD, the absorption peak at 98.9 eV corresponds to the Si-C, which demonstrates the surface modification of the diatomite with octadecyl groups[39].

Hosted file

image4.emf available at <https://authorea.com/users/697876/articles/685852-octadecyl-and-sulfonyl-modification-of-diatomite-synergistically-improved-the-immobilization-efficiency-of-lipase-and-its-application-in-the-synthesis-of-pine-sterol-esters>

Figure 3 . XPS diagram of diatomite before and after modification (A), XPS Si 2p spectra of Diatomite (B), MD (C), OSMD (D)

Table 1 Relative atomic content of the surface before and after modification

	Si 2p (%)	C 1s (%)	O 1s (%)	N 1s (%)
Diatomite	21.8	15.8	61.8	0.7
MD	10.7	33.4	54.7	1.1
OSMD	11.3	66.1	22.5	0.1

As shown in the DTG results, MD reaches the point of maximum thermal decomposition rate at 362.3°C, which indicates the dehydration of surface hydroxyl groups, which is consistent with the OSMD[40]. OSMD shows another jump discontinuity at 561.8°C, which may be due to the loss of grafted octadecyl and sulfonyl groups[41]. Throughout the process, the overall mass loss of MD was 7.6%, while the overall mass loss of OSMD was 8.6%, this indicated that diatomite was successfully modified, while the support itself has excellent thermal stability.

The contact angle serves as a quantitative indicator of surface wettability, which quantifies the angle formed between the interface of the liquid or vapor and the solid surface. According to the Young-According to the Young-Laplace equation, the morphology of a droplet is influenced by the relative hydrophobic or hydrophilic properties of the material's surface with respect to the liquid. A larger contact angle corresponds to a greater repulsive force exerted by the droplet on the surface, signifying a relatively higher degree of hydrophobicity of the material's surface[24]. As depicted in **Figure 3D (a)**, diatomaceous earth exhibits pronounced hydrophilicity owing to the abundance of surface Si-OH groups[41]. Conversely, the contact angle of OSMD increased to 133.5° following additional octadecyl modification, indicative of its heightened hydrophobicity, which can also support that the successful modification of octadecyl.

Figure 4 . TG of MD and OSMD (A), DTG of MD (B) and OSMD (C), the contact angle of MD and OSMD (D)

3.2 Optimization of the ratio of modifiers and surfactants

Although different modification degrees of modifiers ($-\text{SO}_3\text{H}$ and $-\text{C}_{18}$) can result in distinct properties of the carrier and thereby impact its immobilization efficiency, quantitatively analyzing the modification degree can be exceedingly challenging. Thus, to further investigate the effect of the modification degree on the immobilization efficiency and to design a more efficient immobilization carrier, we used the immobilization effect of CRL as an indicator to optimize the modification degree. As shown in **Table 2**, the results suggested that the enzyme loading and activity recovery of modified diatomite modified with $-\text{SO}_3\text{H}$ or $-\text{C}_{18}$ alone was

considerably lower than that of -SO₃H/-C₁₈ (1:1) group, which demonstrated that the -SO₃H and -C₁₈ groups may have a synergistic effect. It can be attributed to several factors, on the one side, the long-chain -C₁₈ provided a suitable hydrophobic microenvironment for the lipase via an interfacial activation mechanism, and on the other hand, the -SO₃H groups changed the charge distribution of the lipase surface, resulting in a stronger binding interaction between lipase and carrier, which could reduce the enzyme leakage. In addition, the ratio of the two modifiers had a significant effect on the immobilization effect, and OSMD had the best immobilization effect with an enzyme loading of 74.40 mg·g⁻¹ and an activity recovery of 63.35% at the ratio of -SO₃H/-C₁₈(1:1.5). The specific mechanism needs to be further investigated to find out.

Given the high hydrophobicity of OSMD, the addition of surfactant enhances the dispersion of the support in the phosphate buffer[42, 43]. In addition, the addition of surfactants can also prevent the aggregation of lipase[44]. However, it also should be noted that the surfactants may also play a negative role during immobilization due to the inactivation of lipases. Hence, it becomes crucial to screen the type and concentration of surfactant (**Figure S4**). The results showed that SDS has a detrimental effect on lipase activity. Nonionic surfactants (Triton X-100, Tween 80) yielded favorable results but were slightly inferior to the cationic surfactant (CTAB). Moreover, the impact of different CTAB concentrations on immobilization efficacy was assessed, revealing that at a concentration of 0.50 mM, CRL loading reached 76.3 mg·g⁻¹, with an enzyme activity recovery of 74.7%. The presence of the cationic surfactant may alter the surface charge of the lipase and enhance its electrostatic interactions with the sulfonic acid groups while preventing lipase dimer formation and thus beneficial to the immobilization processes[45, 46].

Table 2 . Effect of modifier ratio on the immobilization effect of OSMD

Modifier ratio	Enzyme loading (mg·g ⁻¹)	Activity recovery (%)
-SO ₃ H	32.62 ± 1.03	32.37 ± 1.68
-SO ₃ H/-C ₁₈ (1:0.5)	56.77 ± 1.57	40.58 ± 0.79
-SO ₃ H/-C ₁₈ (1:1.0)	63.14 ± 1.29	52.16 ± 1.34
-SO ₃ H/-C ₁₈ (1:1.5)	74.40 ± 1.61	63.35 ± 1.48
-SO ₃ H/-C ₁₈ (1:2.0)	65.95 ± 2.12	60.54 ± 1.61
-C ₁₈	60.51 ± 0.66	54.19 ± 0.86
MD	22.88 ± 0.68	24.57 ± 0.85

Conditions of the immobilization process: the reaction was carried out in 0.1 mol·L⁻¹ phosphate buffer (pH 7.0) with enzyme addition of 100 mg·g⁻¹ (mass of support) for 8 h at 30°C.

3.3 Optimization of *Candida rugosa* lipase immobilization conditions

Lipase immobilization efficiency on hydrophobic supports is generally influenced by enzyme concentration (enzyme addition), pH, temperature, and reaction time[47]. In investigating the factor of enzyme addition (**Figure 5. A**), the results showed that the enzyme loading increased with the enzyme addition. However, considering the enzyme is relatively expensive, even though the enzyme loading and activity of the CRL@OSMD were still slightly increased at more than 100 mg·g⁻¹, the optimum enzyme addition was set to 100 mg·g⁻¹. As shown in **Figure 5. B**, the higher temperature would increase the collision between enzyme molecules and support, thus improving the immobilization rate, but too high temperature will also affect the stability of enzymes in the buffer solution. Taking the CRL loading and enzyme activity together as the evaluation index, 30°C was finally selected as the optimal immobilization temperature.

The pH of the buffer solution affects the surface charge of the CRL (**Figure 5. C**), which in turn affects the electrostatic interaction of the enzyme protein with the sulfonic acid groups in the support. The results showed that the immobilization efficiency and enzyme activity were significantly increased at pH 6.5, indicating that the amino group of CRL is more likely to interact electrostatically with the sulfonic acid group after ion exchange under weakly acidic conditions.

Finally, the time was optimized and the results showed that the longer the immobilization process (**Figure 5.D**), the higher the loading of CRL@OSMD, but by 10 h later, the support was saturated. Continued increase in time, on the contrary, led to a decrease in enzyme activity.

Finally, immobilized CRL with a loading of $84.8 \text{ mg}\cdot\text{g}^{-1}$ and enzyme activity of $54 \text{ U}\cdot\text{g}^{-1}$ was obtained after the reaction at 30°C for 10 h in phosphate buffer at pH 6.5 with an enzyme addition of $100 \text{ mg}\cdot\text{g}^{-1}$, which is significantly higher than that of some previous studies. For instance, Cabrera et al. studied the immobilization of CALB in a series of hydrophobic supports and found that only $30 \text{ mg}\cdot\text{g}^{-1}$ loading was obtained with octadecyl resin as the support[48]. Similarly, Kurtovic et al. adsorbed CRL onto a highly hydrophobic octadecyl methacrylate resin by interfacial activation and only obtained an immobilized enzyme with a loading of $58.7 \text{ mg}\cdot\text{g}^{-1}$ [49]. Thus, in contrast to many existing reports, OSMD exhibited its extreme advantages in enzyme loading.

Figure 5. Optimization of immobilization enzyme addition (A), temperature (B), pH (C), and time (D) of CRL@OSMD

3.4 The stability study of immobilized CRL

To investigate the effect of temperature on CRL@OSMD, the residual enzyme activity of free CRL and CRL@OSMD at 50°C and 60°C were measured with the p-NPP assay. As illustrated in **Figure S5**, as the temperature increased, the residual activity of both free CRL and CRL@OSMD exhibited a diminishing trend. However, it is noteworthy that the relative activity of CRL@OSMD remained conspicuously higher than that of free CRL. These findings suggested that under the experimental conditions, both CRL@OSMD and free CRL retained their activities at levels exceeding 90% when subjected to a 50°C treatment for 1 h. **Figure S5** shows that the residual activity of free CRL and CRL@OSMD decreased with increasing temperature, but the relative activity of CRL@OSMD was significantly higher than that of free CRL. The results indicated that both the activity of CRL@OSMD and free CRL can be maintained above 90% at 50°C treatment for 1 h. However, when the temperature was increased to 60°C , a more pronounced decline in the activity of free CRL was observed, which may be due to the irreversible denaturation and inactivation of the secondary structure of CRL by the higher temperature. In stark contrast, CRL@OSMD exhibited remarkable resilience, maintaining its activity above 80% even after 30 minutes of exposure to the heightened temperature of 60°C . This observation serves as compelling evidence that CRL@OSMD boasts superior thermal stability compared to its free counterpart under the specified experimental conditions.

To investigate the storage stability of the immobilized enzyme, free CRL and immobilized CRL (CRL@OSMD) were stored at 4°C for one month and residual enzyme activity was tested every 5 days at the respective optimum pH and temperature and the initial enzyme activity was defined as 100%. As shown in **Figure S5**, the enzyme activity of free CRL decreased rapidly to less than 50.0% after 10 days, and only 11.3% residual enzyme activity can be maintained after 30 days. In contrast, the storage stability of the OSMD immobilized enzyme was significantly higher than free CRL. After 5 days of storage, 93.2% of the initial enzyme activity was still preserved, and this level of activity endured above 50.0% even after the 30-day storage duration. These results unequivocally underscore the outstanding storage characteristics of the immobilized enzyme, highlighting its impressive reusability and ability to endure extended storage periods, making it well-suited to meet the demands of production requirements.

When p-NPP was used as a model substrate to test the repetitive hydrolysis activity of the immobilized enzyme, it was found that the hydrolysis effect of CRL@OSMD could still reach 86.2% after 10 times of reuse (**Figure S6**), which indicated that the immobilized enzyme had good operational stability and repetitive use performance.

3.5 Synthesis of pine sterol oleate with OSMD@CRL in a solvent-free system

Oleic acid, as a common monounsaturated ω -9 fatty acid, works synergistically with phytosterols to regulate blood lipid levels and effectively reduce hypercholesterolemia and cardiovascular disease[50]. In addition, our previous studies also found that oleic acid is one of the most efficient substrates for the esterification

reaction due to its low melting point and its high solubility of phytosterols[50] (**Figure 6**). With excess oleic acid as a solvent, the additional costs and environmental concerns associated with the use of organic solvents can be avoided[51, 52]. Optimization of solvent-free esterification involves obtaining high conversions while avoiding excess reagents and catalysts and saving energy[53]. However, solvent-free reactions present specific challenges given the drastic changes that can occur in the reaction medium during the reaction processes[54]. Specific studies are needed to determine the optimal amounts of reagents and catalysts and the optimal temperatures under these conditions, where the thermodynamic and kinetic aspects converge toward high conversion[50].

Most enzymatic esterification studies consider the molar ratio of reagents, biocatalyst addition, reaction time, and temperature as the main variables that determine the reaction yield[50]. Moreover, there are two possible strategies to change the esterification equilibrium: (1) use an excess amount of one of the reagents or (2) remove one of the product mediators (water) from the reaction[55]. As the relatively low cost of oleic acid and it can act as the solvent of the solvent-free system, the ratio of oleic acid: pine sterol was selected from 1:4 to 1:8. As shown in the results of **Figure 6. A** , the yield can only reach 53.4% and 65.7% at ratios of 1:4 and 1:5 which can largely be attributed to the incomplete dissolution of pine sterol in the reaction medium. Nonetheless, it's worth noting that excessive quantities of oleic acid can also exert a detrimental influence on esterification efficiency. This is likely attributable to a reduction in the relative concentration of pine sterol within the oleic acid medium, leading to a diminished likelihood of substrate access to the enzyme's active center. The optimal esterification yield was achieved when the molar ratio of pine sterol to oleic acid was maintained at 1:6. This ratio takes into consideration the intricate dynamics introduced by the reaction medium, resulting in the highest efficiency.

The amount of biocatalyst in the reaction is limited by the dispersing capacity of the stirring system and the filtration capacity of the system[56-58]. The amount of enzyme addition in the system does not affect the final yield of the ester in equilibrium, but it does affect the reaction rate. Reaction product-induced lipase inhibition may occur under specific circumstances of the reaction[55, 59]. As shown in the results of **Figure 6. B** , the lower yield of the reaction at an enzyme addition of $5.0 \text{ U}\cdot\text{g}^{-1}$ (relative to the mass of pine sterol) is most likely due to a decrease in the rate of the reaction, as well as product inhibition. The efficiency of the esterification reaction remained essentially the same at enzyme additions above $8.0 \text{ U}\cdot\text{g}^{-1}$, which was finally chosen given the high cost of biocatalysts.

The temperature has a positive effect on the energy of the reagents, favoring the effective number of collisions leading to product formation[60-62]. However, collateral effects may occur - high temperatures may cause conformational changes in the enzyme, leading to an increase (or loss) of enzyme catalytic activity[61, 63]. Thus, incremental increases in reaction kinetics due to increased temperatures may be offset by reductions in the catalytic activity of lipases[64]. Temperature also affects the solubility of the reagents and viscosity reduction, which means that there are considerable changes in the reaction medium, and these changes affect the apparent equilibrium position because only dissolved reactants are involved in the thermodynamic process, and only dissolved substrates can be contacted by the enzyme[65]. The optimal temperature for enzymatic esterification should facilitate proper diffusion of the reagents in the medium, thus maintaining the performance of the biocatalyst. As shown in **Figure 6. C** , the low yield at 35°C was attributed to the poor solubilization of the pine sterols and the high mass transfer resistance of the medium due to the high viscosity of oleic acid at a low temperature, which resulted in the diffusion of substrates to the active site of CRL@OSMD became more difficult. In addition, the temperature above 55°C may also have a negative effect on the esterification yield due to the denature of CRL@OSMD. Taking into account the catalytic activity of the immobilized enzyme and the efficiency of the esterification reaction, 50°C was finally selected as the optimum reaction temperature. Reaction time affects the efficiency of product production and reduces the number of times the biocatalyst can be recycled, and reaching reaction equilibrium cannot always be pursued to maximize the benefits of immobilized enzyme-catalyzed esterification. The esterification reaction yield can reach 95.0% at 48 h (**Figure 6.D**), and further increasing the reaction time did not have a significant effect on the esterification yield. Moreover, only a conversion of 91.1% of phytosterols can be obtained even though the dry air was introduced to regulate water activity at 72 h[66], which may increase the production cost.

Fortunately, in this study, we found that our modified diatomite with long-chain alkyls, namely OSMD, can prevent the water molecules from adhering to the surface and thus beneficial to the reaction without dry air treatment.

Figure 6. Optimization of molar ratio (A), enzyme addition (B), temperature (C) and time (D) of the esterification reaction

3.6 Substrate scope investigation of immobilized CRL

To investigate the substrate scope of the immobilized lipase (CRL@OSMD), several medium or long-chain fatty acids, such as linoleic acid (C18:2), linolenic acid (C18:3), lauric acid (C12:0), and decanoic acid (C10:0) were selected as the acyl donors. As summarized in **Table 3**, both saturated and unsaturated fatty acids can be used as the acyl donors of the esterification of pine sterol with phytosterol conversions at close to or above 90%. However, as the high melting point of the long-chain (above C12) saturated fatty acids are not beneficial to the solubility of pine sterol and the transfer mass effect of the reactions, only lauric acid and decanoic acid were selected as the model of saturated fatty acid with a yield of $92.33 \pm 1.29\%$ and $90.45 \pm 1.70\%$. To further promote the industrial production processes, edible oil, which contains oleic acid, linoleic acid, and linolenic acid was also selected as the substrate in the synthesis of pine sterol esters, and the results showed that the yield can reach as high as $94.14 \pm 1.37\%$. This indicates that our novel-designed immobilized enzyme (CRL@OSMD) can catalyze the esterification reaction of pine sterols with excellent substrate applicability, which can be adapted to the needs of processing and production.

Table 3. Substrate scope investigation

Fatty Acid	Conversion rate (%)
Oleic acid (C18:1) ^b	95.01 ± 0.87
Linoleic acid (C18:2)	94.50 ± 0.93
Linolenic acid (C18:3)	93.80 ± 0.49
Lauric acid (C12:0)	90.45 ± 1.70
Decanoic acid (C10:0)	92.33 ± 1.29
Mixed acids	94.14 ± 1.37

^a Reaction conditions: 1 mmol pine sterol, 6 mmol fatty acid, 8 U/g (based on the mass of pine sterol) CRL@OSMD, 50°C, 48 h.

^b The first number in parentheses represents the number of carbon atoms of the fatty acid, and the second number represents the number of carbon-carbon double bonds of the fatty acid.

^c Mixing oleic, linoleic, and linolenic acids in equimolar ratios to simulate edible oils.

3.7 Process scale-up and reusability studies

To explore the scalability of the pine sterol ester synthesis process developed above, the amount of substrate was scaled up to 10 times, and a final esterification of 94.3% of pine sterol ester was obtained, demonstrating the scalable production potential of the new process for the synthesis of pine sterol esters catalyzed by the immobilized enzymes in the study. Moreover, the reusability of the catalyst was investigated under the optimized conditions, and the results are shown in **Figure S6**. It can be seen that the esterification yield decreased with the increase of cycles, and could still be maintained above 70.9% after 6 cycles. The decrease in esterification yield is most likely due to the unavoidable loss of the immobilized enzyme during the separation from the reaction system, as well as denaturation and inactivation of the enzyme during the reaction. For instance, Zhang et al. suggested that only 82.0% activity of CRL immobilized with a hollow cubic carbon can be maintained in the second cycle[67]. However, in this study, our novel-designed OSMD immobilization can maintain the residual activity as high as 90.6% in two cycles, which suggests that the

novel-designed OSMD in this study is a good candidate in lipase immobilization and has great potential for application in further food biomanufacturing.

4. Conclusion

A low-cost and designable material, namely diatomite, was investigated in the immobilization of CRL and then used for the synthesis of various pine sterol esters. To further improve its efficiency, sulfonyl and octadecyl were employed as modifiers to regulate the hydrophobicity and the binding interaction between support and lipase. In addition, the Fe_3O_4 was also introduced to this system for quick and simple separation via the magnetic field. Interestingly, the enzyme loading and activity recovery of the single modification diatomite via octadecyl or sulfonyl group was lower than that of two functional groups modification diatomite, namely OSMD. It indicated that there may be a synergistic effect between these two modifiers, the octadecyl modification endowed a suitable hydrophobicity of diatomite, and the sulfonyl group changed the interaction between lipase and support which enhanced the enzyme loading of CRL. The optimization of the ratio of the modifiers suggested that the $-\text{SO}_3\text{H}/\text{C}_{18}$ (1:1.5) performed best with an enzyme loading and enzyme activity of $84.8 \text{ mg}\cdot\text{g}^{-1}$ and $54 \text{ U}\cdot\text{g}^{-1}$, respectively. Compared to free CRL, the thermal and storage stability of CRL@OSMD was significantly improved, which lays the foundation for the catalytic synthesis of phytosterol esters in a solvent-free system. The molar ratio of pine sterol and oleic acid, enzyme addition, reaction temperature, and time in the esterification reaction were optimized, and finally the reaction was carried out at a molar ratio of pine sterol to oleic acid of 1:6, an enzyme addition of $8.0 \text{ U}\cdot\text{g}^{-1}$ (concerning the mass of pine sterol), and at a temperature of 50°C for 48 h, which could ultimately achieve an esterification yield of 95.0%. After cycling the reaction 6 times, the esterification yield still reached more than 70.0%. This study shows that OSMD materials are good candidates for lipase immobilization and have great potential for application in further food biomanufacturing with low-cost and high efficiency.

ACKNOWLEDGEMENT

This research was financially supported by the National key R&D program of China (No.2021YFC2103800), National Natural Science Foundation of China (No. 22178174), Jiangsu Synergetic Innovation Center for Advanced Bio-Manufacture (XTC2206).

AUTHOR INFORMATION

Corresponding author:

Yi Hu, E-mail:huyi@njtech.edu.cn; Binbin Nian, E-mail:bbnian@njtech.edu.cn.

Notes

The authors declare no competing financial interests.

References:

- [1] Lagarda, M., García-Llatas, G., Farré, R., Analysis of phytosterols in foods. *Journal of pharmaceutical and biomedical analysis* 2006, *41* , 1486-1496.
- [2] Weete, J. D., Abril, M., Blackwell, M., Phylogenetic distribution of fungal sterols. *PloS one* 2010, *5* , e10899.
- [3] Michellod, D., Bien, T., Birgel, D., Violette, M., *et al.* , De novo phytosterol synthesis in animals. *Science* 2023, *380* , 520-526.
- [4] Piironen, V., Lindsay, D. G., Miettinen, T. A., Toivo, J., Lampi, A. M., Plant sterols: biosynthesis, biological function and their importance to human nutrition. *Journal of the Science of Food and Agriculture* 2000, *80* , 939-966.
- [5] Salehi-Sahlabadi, A., Varkaneh, H. K., Shahdadian, F., Ghaedi, E., *et al.* , Effects of Phytosterols supplementation on blood glucose, glycosylated hemoglobin (HbA1c) and insulin levels in humans: a systematic

review and meta-analysis of randomized controlled trials. *Journal of Diabetes & Metabolic Disorders* 2020, *19* , 625-632.

[6] Moreau, R. A., Whitaker, B. D., Hicks, K. B., Phytosterols, phytostanols, and their conjugates in foods: structural diversity, quantitative analysis, and health-promoting uses. *Progress in lipid research* 2002, *41* , 457-500.

[7] Bacchetti, T., Masciangelo, S., Bicchiega, V., Bertoli, E., Ferretti, G., Phytosterols, phytostanols and their esters: from natural to functional foods. *Mediterranean Journal of Nutrition and Metabolism* 2011, *4* , 165-172.

[8] Dash, R., Mitra, S., Ali, M. C., Oktaviani, D. F., *et al.* , Phytosterols: Targeting neuroinflammation in neurodegeneration. *Current Pharmaceutical Design* 2021, *27* , 383-401.

[9] Hannan, M. A., Sohag, A. A. M., Dash, R., Haque, M. N., *et al.* , Phytosterols of marine algae: Insights into the potential health benefits and molecular pharmacology. *Phytomedicine* 2020, *69* , 153201.

[10] Kuryłowicz, A., Cakała-Jakimowicz, M., Puzianowska-Kuźnicka, M., Targeting abdominal obesity and its complications with dietary phytoestrogens. *Nutrients* 2020, *12* , 582.

[11] Burčová, Z., Kreps, F., Greifová, M., Jablonský, M., *et al.* , Antibacterial and antifungal activity of phytosterols and methyl dehydroabietate of Norway spruce bark extracts. *Journal of biotechnology* 2018, *282* , 18-24.

[12] Chen, L., Deng, H., Cui, H., Fang, J., *et al.* , Inflammatory responses and inflammation-associated diseases in organs. *Oncotarget* 2018, *9* , 7204.

[13] Scolaro, B., Andrade, L. F. d., Castro, I. A., Cardiovascular disease prevention: The earlier the better? A review of plant sterol metabolism and implications of childhood supplementation. *International Journal of Molecular Sciences* 2019, *21* , 128.

[14] Ramprasath, V. R., Awad, A. B., Role of phytosterols in cancer prevention and treatment. *Journal of AOAC International* 2015, *98* , 735-738.

[15] Suttiarporn, P., Chumpolsri, W., Mahatheeranont, S., Luangkamin, S., *et al.* , Structures of phytosterols and triterpenoids with potential anti-cancer activity in bran of black non-glutinous rice. *Nutrients* 2015, *7* , 1672-1687.

[16] Yang, Y., He, W., Jia, C., Ma, Y., *et al.* , Efficient synthesis of phytosteryl esters using the Lewis acidic ionic liquid. *Journal of Molecular Catalysis A: Chemical* 2012, *357* , 39-43.

[17] Tan, Z., Le, K., Moghadasian, M., Shahidi, F., Enzymatic synthesis of phytosteryl docosahexaneates and evaluation of their anti-atherogenic effects in apo-E deficient mice. *Food chemistry* 2012, *134* , 2097-2104.

[18] Shi, H., Li, S., Liu, J., Wang, S., *et al.* , Green and efficient synthesis of pine sterol oleate catalyzed by SO₃H-functionalized ionic liquid. *Journal of Chemical Technology & Biotechnology* 2022, *97* , 3083-3090.

[19] Lortie, R., Enzyme catalyzed esterification. *Biotechnology Advances* 1997, *15* , 1-15.

[20] Maldonado, R. R., Burkert, J. F. M., Mazutti, M. A., Maugeri, F., Rodrigues, M. I., Evaluation of lipase production by *Geotrichum candidum* in shaken flasks and bench-scale stirred bioreactor using different impellers. *Biocatalysis and Agricultural Biotechnology* 2012, *1* , 147-151.

[21] Zheng, M.-M., Lu, Y., Dong, L., Guo, P.-M., *et al.* , Immobilization of *Candida rugosa* lipase on hydrophobic/strong cation-exchange functional silica particles for biocatalytic synthesis of phytosterol esters. *Bioresource Technology* 2012, *115* , 141-146.

[22] Zeng, C., Qi, S., Li, Z., Luo, R., *et al.* , Enzymatic synthesis of phytosterol esters catalyzed by *Candida rugosa* lipase in water-in-[Bmim]PF₆ microemulsion. *Bioprocess and biosystems engineering* 2015, *38* , 939-946.

- [23] Hu, L., Llibin, S., Li, J., Qi, L., *et al.* , Lipase-catalyzed transesterification of soybean oil and phytosterol in supercritical CO₂. *Bioprocess and biosystems engineering* 2015, *38* , 2343-2347.
- [24] Chen, B., Jia, Y., Zhang, M., Li, X., *et al.* , Facile modification of sepiolite and its application in superhydrophobic coatings. *Applied Clay Science* 2019, *174* , 1-9.
- [25] Cabrera, M. P., da Fonseca, T. F., de Souza, R. V. B., de Assis, C. R. D., *et al.* , Polyaniline-coated magnetic diatomite nanoparticles as a matrix for immobilizing enzymes. *Applied Surface Science* 2018, *457* , 21-29.
- [26] Zhao, K., Cao, X., Di, Q., Wang, M., *et al.* , Synthesis, characterization and optimization of a two-step immobilized lipase. *Renewable energy* 2017, *103* , 383-387.
- [27] Tran, D.-T., Chen, C.-L., Chang, J.-S., Continuous biodiesel conversion via enzymatic transesterification catalyzed by immobilized Burkholderia lipase in a packed-bed bioreactor. *Applied Energy* 2016, *168* , 340-350.
- [28] Basso, A., Hesseler, M., Serban, S., Hydrophobic microenvironment optimization for efficient immobilization of lipases on octadecyl functionalised resins. *Tetrahedron* 2016, *72* , 7323-7328.
- [29] Singh, A. K., Mukhopadhyay, M., Immobilization of lipase on carboxylic acid-modified silica nanoparticles for olive oil glycerolysis. *Bioprocess and biosystems engineering* 2018, *41* , 115-127.
- [30] Fu, D., Li, C., Lu, J., ur Rahman, A., Tan, T., Relationship between thermal inactivation and conformational change of *Yarrowia lipolytica* lipase and the effect of additives on enzyme stability. *Journal of Molecular Catalysis B: Enzymatic* 2010, *66* , 136-141.
- [31] Hilterhaus, L., Thum, O., Liese, A., Reactor concept for lipase-catalyzed solvent-free conversion of highly viscous reactants forming two-phase systems. *Organic Process Research & Development* 2008, *12* , 618-625.
- [32] Boudrant, J., Woodley, J. M., Fernandez-Lafuente, R., Parameters necessary to define an immobilized enzyme preparation. *Process Biochemistry* 2020, *90* , 66-80.
- [33] Guo, J., Chen, C.-P., Wang, S.-G., Huang, X.-J., A convenient test for lipase activity in aqueous-based solutions. *Enzyme and Microbial Technology* 2015, *71* , 8-12.
- [34] Pencreac'h, G., Baratti, J. C., Activity of *Pseudomonas cepacia* lipase in organic media is greatly enhanced after immobilization on a polypropylene support. *Applied Microbiology and Biotechnology* 1997, *47* , 630-635.
- [35] Li, Y., Li, B., Zhao, X., Tian, N., Zhang, J., Totally waterborne, nonfluorinated, mechanically robust, and self-healing superhydrophobic coatings for actual anti-icing. *ACS applied materials & interfaces* 2018, *10* , 39391-39399.
- [36] Xu, F., Li, D., Chen, W., Gao, S., Formation of hydrophobic silica coatings on stones for conservation of historic sculptures. *Chinese Journal of Chemistry* 2010, *28* , 1487-1490.
- [37] Zhang, W., Zhang, Y., Lu, Z., Nian, B., *et al.* , Enhanced stability and catalytic performance of laccase immobilized on magnetic graphene oxide modified with ionic liquids. *Journal of Environmental Management* 2023, *346* , 118975.
- [38] Feng, K., Hung, G.-Y., Liu, J., Li, M., *et al.* , Fabrication of high performance superhydrophobic coatings by spray-coating of polysiloxane modified halloysite nanotubes. *Chemical Engineering Journal* 2018, *331* , 744-754.
- [39] Wu, S., Wang, C., Jin, Y., Zhou, G., *et al.* , Green synthesis of reusable super-paramagnetic diatomite for aqueous nickel (II) removal. *Journal of Colloid and Interface Science* 2021, *582* , 1179-1190.
- [40] Peng, X., Yuan, Z., Zhao, H., Wang, H., Wang, X., Preparation and mechanism of hydrophobic modified diatomite coatings for oil-water separation. *Separation and Purification Technology* 2022, *288* , 120708.

- [41] Zhang, Y., Zhang, J., Wang, A., From Maya blue to biomimetic pigments: durable biomimetic pigments with self-cleaning property. *Journal of Materials Chemistry A* 2016, *4* , 901-907.
- [42] Fernández-Lorente, G., Palomo, J. M., Fuentes, M., Mateo, C., *et al.* , Self-assembly of *Pseudomonas fluorescens* lipase into bimolecular aggregates dramatically affects functional properties. *Biotechnology and bioengineering* 2003, *82* , 232-237.
- [43] Martins, A. B., Friedrich, J. L., Cavalheiro, J. C., Garcia-Galan, C., *et al.* , Improved production of butyl butyrate with lipase from *Thermomyces lanuginosus* immobilized on styrene–divinylbenzene beads. *Bioresource technology* 2013, *134* , 417-422.
- [44] Wiemann, L. O., Nieguth, R., Eckstein, M., Naumann, M., *et al.* , Composite particles of novozyme 435 and silicone: advancing technical applicability of macroporous enzyme carriers. *ChemCatChem* 2009, *1* , 455-462.
- [45] dos Santos, J. C., Garcia-Galan, C., Rodrigues, R. C., de Sant’Ana, H. B., *et al.* , Stabilizing hyperactivated lecithase structures through physical treatment with ionic polymers. *Process Biochemistry* 2014, *49* , 1511-1515.
- [46] Santos, J. C. S. d., Barbosa, O., Ortiz, C., Berenguer-Murcia, A., *et al.* , Importance of the support properties for immobilization or purification of enzymes. *ChemCatChem* 2015, *7* , 2413-2432.
- [47] Rodrigues, R. C., Virgen-Ortiz, J. J., Dos Santos, J. C., Berenguer-Murcia, A., *et al.* , Immobilization of lipases on hydrophobic supports: immobilization mechanism, advantages, problems, and solutions. *Biotechnology Advances* 2019, *37* , 746-770.
- [48] Verdasco-Martin, C. M., Garcia-Verdugo, E., Porcar, R., Fernandez-Lafuente, R., Otero, C., Selective synthesis of partial glycerides of conjugated linoleic acids via modulation of the catalytic properties of lipases by immobilization on different supports. *Food Chemistry* 2018, *245* , 39-46.
- [49] Kurtovic, I., Nalder, T. D., Cleaver, H., Marshall, S. N., Immobilisation of *Candida rugosa* lipase on a highly hydrophobic support: A stable immobilised lipase suitable for non-aqueous synthesis. *Biotechnology Reports* 2020, *28* , e00535.
- [50] Sousa, R. R., Silva, A. S. A., Fernandez-Lafuente, R., Ferreira-Leitao, V. S., Solvent-free esterifications mediated by immobilized lipases: A review from thermodynamic and kinetic perspectives. *Catalysis Science & Technology* 2021, *11* , 5696-5711.
- [51] Hari Krishna, S., Karanth, N., Lipases and lipase-catalyzed esterification reactions in nonaqueous media. *Catalysis Reviews* 2002, *44* , 499-591.
- [52] Dossat, V., Combes, D., Marty, A., Lipase-catalysed transesterification of high oleic sunflower oil. *Enzyme and Microbial Technology* 2002, *30* , 90-94.
- [53] Ghamgui, H., Karra-Chaabouni, M., Gargouri, Y., 1-Butyl oleate synthesis by immobilized lipase from *Rhizopus oryzae*: a comparative study between n-hexane and solvent-free system. *Enzyme and Microbial Technology* 2004, *35* , 355-363.
- [54] Sandoval, G., Condoret, J., Monsan, P., Marty, A., Esterification by immobilized lipase in solvent-free media: Kinetic and thermodynamic arguments. *Biotechnology and bioengineering* 2002, *78* , 313-320.
- [55] Castillo, E., Torres-Gavilan, A., Sandoval, G., Marty, A., Thermodynamical methods for the optimization of lipase-catalyzed reactions. *Lipases and Phospholipases: Methods and Protocols* 2012, 383-400.
- [56] Adlercreutz, P., Immobilisation and application of lipases in organic media. *Chemical Society Reviews* 2013, *42* , 6406-6436.
- [57] Goldberg, M., Thomas, D., Legoy, M.-D., Water activity as a key parameter of synthesis reactions: the example of lipase in biphasic (liquid/solid) media. *Enzyme and microbial technology* 1990, *12* , 976-981.

- [58] Colombie, S., Tweddell, R. J., Condoret, J. S., Marty, A., Water activity control: A way to improve the efficiency of continuous lipase esterification. *Biotechnology and bioengineering* 1998,60 , 362-368.
- [59] Lopresto, C. G., Calabro, V., Woodley, J. M., Tufvesson, P., Kinetic study on the enzymatic esterification of octanoic acid and hexanol by immobilized *Candida antarctica* lipase B. *Journal of Molecular Catalysis B: Enzymatic* 2014, 110 , 64-71.
- [60] Vadgama, R. N., Odaneth, A. A., Lali, A. M., Green synthesis of isopropyl myristate in novel single phase medium Part I: Batch optimization studies. *Biotechnology Reports* 2015, 8 , 133-137.
- [61] Kuperkar, V. V., Lade, V. G., Prakash, A., Rathod, V. K., Synthesis of isobutyl propionate using immobilized lipase in a solvent free system: optimization and kinetic studies. *Journal of Molecular Catalysis B: Enzymatic* 2014, 99 , 143-149.
- [62] Scillipoti, J., Nioi, C., Marty, A., Camy, S., Condoret, J.-S., Prediction of conversion at equilibrium for lipase esterification in two-phase systems. *Biochemical engineering journal* 2017,117 , 162-171.
- [63] Martins, A. B., Schein, M. F., Friedrich, J. L., Fernandez-Lafuente, R., *et al.* , Ultrasound-assisted butyl acetate synthesis catalyzed by Novozym 435: Enhanced activity and operational stability. *Ultrasonics sonochemistry* 2013, 20 , 1155-1160.
- [64] Romero, M., Calvo, L., Alba, C., Daneshfar, A., Ghaziaskar, H., Enzymatic synthesis of isoamyl acetate with immobilized *Candida antarctica* lipase in n-hexane. *Enzyme and microbial technology*2005, 37 , 42-48.
- [65] Khan, N. R., Rathod, V. K., Enzyme catalyzed synthesis of cosmetic esters and its intensification: A review. *Process Biochemistry* 2015, 50 , 1793-1806.
- [66] Cui, C., Guan, N., Xing, C., Chen, B., Tan, T., Immobilization of *Yarrowia lipolytica* lipase Ylip2 for the biocatalytic synthesis of phytosterol ester in a water activity controlled reactor. *Colloids and Surfaces B: Biointerfaces* 2016, 146 , 490-497.
- [67] Zhang, S., Hou, H., Zhao, B., Zhou, Q., *et al.* , Hollow mesoporous carbon-based enzyme nanoreactor for the confined and interfacial biocatalytic synthesis of phytosterol esters. *Journal of Agricultural and Food Chemistry* 2023, 71 , 2014-2025.

Hosted file

Graphics.docx available at <https://authorea.com/users/697876/articles/685852-octadecyl-and-sulfonyl-modification-of-diatomite-synergistically-improved-the-immobilization-efficiency-of-lipase-and-its-application-in-the-synthesis-of-pine-sterol-esters>